

О СРАВНЕНИИ МЕХАНИЗМОВ РЕАКТИВНО-ИОННОГО ТРАВЛЕНИЯ SiO₂ ВО ФТОР- И ХЛОРСОДЕРЖАЩЕЙ ПЛАЗМЕ

А.М. Ефремов, С.А. Смирнов, В.Б. Бетелин, К.-Н. Kwon

Александр Михайлович Ефремов (ORCID 0000-0002-9125-0763)*, Сергей Александрович Смирнов (ORCID 0000-0002-0375-0494)

Ивановский государственный химико-технологический университет, Шереметевский просп., 7, Иваново, Российская Федерация, 153000

E-mail: amefremov@mail.ru*, sas@isuct.ru

Владимир Борисович Бетелин (ORCID 0000-0001-6646-2660)

ФГУ ФНЦ НИИСИ РАН, Нахимовский просп., 36, к.1, Москва, Российская Федерация, 117218

E-mail: betelin@niisi.msk.ru

Kwang-Ho Kwon (ORCID 0000-0003-2580-8842)

Korea University, 208 Seochang-Dong, Chochiwon, Korea, 339-800

E-mail: kwonkh@korea.ac.kr

Исследовано влияние соотношения компонентов, вкладываемой мощности и давления газа на электрофизические параметры плазмы, стационарные концентрации активных частиц и кинетику реактивно-ионного травления SiO₂ в смесях CF₄ + Ar и Cl₂ + Ar. При совместном использовании методов зондовой диагностики и моделирования плазмы установлено, что варьирование внешних параметров приводит к однотипным изменениям интенсивностей физического и химического факторов, определяющих скорость реактивно-ионного травления (РИТ) SiO₂ в каждой из систем. Единственным исключением является противоположное влияние давления газа на плотность потока атомов фтора и хлора. Проведен анализ кинетики РИТ с использованием расчетных данных по плотностям потоков ионов и химически активных частиц. Установлено, что доминирующим механизмом травления в обеих смесях является гетерогенная химическая реакция, скорость которой коррелирует с изменением плотности потока атомов фтора или хлора. Эффективная вероятность реакции Si + nF → SiF_n снижается с ростом интенсивности ионной бомбардировки поверхности. Такая ситуация характерна для отсутствия ионно-лимитируемых стадий травления, при этом отрицательный эффект ионной бомбардировки может быть обусловлен десорбцией атомов фтора в условиях высоких степеней заполнения поверхности адсорбированными частицами и преимущественно спонтанного характера взаимодействия. Эффективная вероятность реакции Si + nCl → SiCl_n характеризуется значительно более низкими абсолютными значениями и симбатным изменением по отношению к интенсивности ионной бомбардировки. Это указывает на ионно-стимулированный механизм химического взаимодействия, проявляющийся, вероятно, через очистку и/или образование центров адсорбции для атомов хлора.

Ключевые слова: CF₄, Cl₂, плазма, параметры, активные частицы, ионизация, диссоциация, травление, кинетика, механизм

Для цитирования:

Ефремов А.М., Смирнов С.А., Бетелин В.Б., Kwon К.-Н. О сравнении механизмов реактивно-ионного травления SiO₂ во фтор- и хлорсодержащей плазме. *Изв. вузов. Химия и хим. технология.* 2023. Т. 66. Вып. 8 С. 54–62. DOI: 10.6060/ivkkt.20236608.6746.

For citation:

Efremov A.M., Smirnov S.A., Betelin V.B., Kwon K.-H. On the comparison of reactive-ion etching mechanisms for SiO₂ in fluorine- and chlorine-containing plasmas. *ChemChemTech [Izv. Vyssh. Uchebn. Zaved. Khim. Khim. Tekhnol.]*. 2023. V. 66. N 8. P. 54–62. DOI: 10.6060/ivkkt.20236608.6746.

ON THE COMPARISON OF REACTIVE-ION ETCHING MECHANISMS FOR SiO₂ IN FLUORINE- AND CHLORINE-CONTAINING PLASMAS

A.M. Efremov, S.A. Smirnov, V.B. Betelin, K.-H. Kwon

Alexander M. Efremov (ORCID 0000-0002-9125-0763)*, Sergey A. Smirnov (ORCID 0000-0002-0375-0494)

Ivanovo State University of Chemistry and Technology, Sheremetevskiy ave., 7, Ivanovo, 153000, Russia

E-mail: amefremov@mail.ru*, sas@isuct.ru

Vladimir B. Betelin (ORCID 0000-0001-6646-2660)

SRISA RAS, Nakhimovskiy ave., 36, bld. 1, Moscow, 117218, Russia

E-mail: betelin@niisi.msk.ru

Kwang-Ho Kwon (ORCID 0000-0003-2580-8842)

Korea University, 208 Seochang-Dong, Chochiwon, Korea, 339-800

E-mail: kwonkh@korea.ac.kr

This work investigated the influence of component ratio, input power and gas pressure on electro-physical plasma parameters, steady-state densities of active species and reactive-ion etching kinetics for SiO₂ in CF₄ + Ar and Cl₂ + Ar plasmas. The combination of plasma diagnostics by Langmuir probes and plasma modeling indicated that the variation of processing conditions causes similar changes in physical and chemical factors influencing the reactive-ion etching (RIE) rate for SiO₂. The only one exception is the opposite effect of gas pressure on densities of fluorine and chlorine atoms. The analysis of RIE kinetics was carried out using model-predicted data on fluxes of ions and chemically active species. It was found that the dominant etching mechanism in both gas mixtures is the heterogeneous chemical reaction while the reaction rate correlates with fluxes of fluorine or chlorine atoms. The effective probability for the $\text{Si} + n\text{F} \rightarrow \text{SiF}_n$ reaction decreases with an increase in the ion bombardment intensity. Such situation reveals no ion-driven limiting stages while the negative effect of ion bombardment may result from desorption of F atoms under conditions of high adsorption degree and spontaneous interaction mechanism. The effective probability for the $\text{Si} + n\text{Cl} \rightarrow \text{SiCl}_n$ reaction exhibits much lower absolute values as well as always traces the change in the ion bombardment intensity. This allows one to assume the ion-assisted reaction regime which is activated by the formation and/or cleaning of adsorption sites for chlorine atoms.

Key words: CF₄, Cl₂, plasma, parameters, active species, ionization, dissociation, etching, kinetics, mechanism

INTRODUCTION

In our days, silicon-based electronics still occupy the dominant position in the worldwide production of integrated electronic circuits. One of key materials in such devices is the silicon dioxide, SiO₂, which is used as gate dielectric for field-effect structures, inter-layer insulator in multi-layer structures, final passivation coating and hard mask in some photolithography procedures [1-3]. Since all these applications assume the precision patterning (dimensional etching) of the preliminary deposited permanent SiO₂ layer, the development of corresponding dry etching processes is an essential problem to be solved for obtaining the desirable device structure and performance. From Refs. [3-5], it can be understood that the most effective tool to obtain nano-scale patterns on SiO₂ is the reactive-ion etching (RIE) technique. This process combines physical and chemical etching pathways which are

closely matched one with each other: the ion bombardment accelerates chemical reactions through breaking bonds between surface atoms and/or desorption of low volatile reaction products while chemical reactions lower the sputter threshold and increase the sputter yield. Accordingly, the adjustment of neutral flux, ion flux and ion bombardment energy provides the effective optimization of etching rate, etching selectivity in respect to the mask material and shapes of etching profiles.

Until now, there were many studies dealt with RIE characteristics of SiO₂ in fluorine- and chlorine-based gas chemistries [2, 4, 6-10]. Principal results of these works related to the process chemistry may briefly be summarized as follows:

- The spontaneous SiO₂(s.) + F/Cl reaction at typical substrate temperatures (below 80 °C in order to provide the stability for the photoresist mask) is thermodynamically forbidden. The reason is that the Si-O

bond (~ 800 kJ/mol) is noticeably stronger compared with Si-F (~ 553 kJ/mol) and Si-Cl (~ 308 kJ/mol) ones [11]. That is why the chemical etching pathway always appears as the ion-assisted process and is initiated by the ion-induced destruction of oxide bonds $\text{SiO}_x(\text{s.}) \rightarrow \text{Si}(\text{s.}) + x\text{O}$, where index (s.) denotes the surface-bonded state of corresponding particle.

- The probability of chemical reaction $\text{Si}(\text{s.}) + x\text{Cl} \rightarrow \text{SiCl}_x(\text{s.})$ is lower compared with $\text{Si}(\text{s.}) + x\text{F} \rightarrow \text{SiF}_x(\text{s.})$. This phenomenon is normally attributed to bigger size of Cl atoms that retard its penetration inside the lattice of etched material. As a result, the etching in chlorine-containing plasmas leads to the formation of non-saturated $\text{SiCl}_x(\text{s.})$ ($x = 1, 2$) compounds where each silicon atom keeps one or even several original bonds with its neighborhood. Therefore, the gasification of reaction products $\text{SiCl}_x(\text{s.}) \rightarrow \text{SiCl}_x$ also needs the ion bombardment and represents, in fact, the chemically activated sputtering process. Oppositely, the etching in fluorine-containing plasmas causes the formation of volatile SiF_4 , and the reaction $\text{SiF}_4(\text{s.}) \rightarrow \text{SiF}_4$ occurs spontaneously at nearly room temperatures.

Though above data explain in general why chlorine-containing plasmas provides lower SiO_2 etching rates together with more anisotropic etching profile, there are several important issues which require additional attention and research efforts. First, the most of mentioned works had the experimental nature and thus, did not analyze the relationships between gas-phase plasma characteristic and heterogeneous process kinetics. Obviously, such situation does not provide the complete understanding of SiO_2 etching mechanisms, especially in respect to contributions physical and chemical etching pathways as well as side factors influencing the ion-assisted chemical reaction. And secondly, previous studies related to fluorine- and chlorine-containing plasmas were made at different processing conditions and in different types of plasma etching reactors. Since corresponding results cannot be compared directly, it is hard to select an appropriate active gas for the given process requirements.

In our previous work [12], we have performed the comparative study of SiO_2 etching kinetics in $\text{CF}_4 + \text{Ar}$ and $\text{Cl}_2 + \text{Ar}$ plasmas under identical processing conditions. Though some reasonable results in respect to both gas-phase and heterogeneous chemistries were obtained, corresponding conclusions have the somewhat limited value for both theoretical and practical aspects. The reasons are that a) only the gas mixing ratio was used as the variable parameter; and b) both experimental and plasma modeling conditions corresponded the negative dc bias voltage of ~ 400 V.

The latter is rather typical for RIE of SiO_2 as a hard mask, but not as the insulating layer. In the last case, the high-energy ion bombardment is strongly undesirable due to the surface damage leading to the degradation of dielectric properties [3, 4].

The main idea of this work was to compare the SiO_2 etching kinetics as well as to analyze corresponding etching mechanisms in $\text{CF}_4 + \text{Ar}$ and $\text{Cl}_2 + \text{Ar}$ plasmas using the extended set of variable inputs (gas mixing ratio, gas pressure and input power) and at lower ion bombardment energies. Accordingly, questions of primary interest were 1) the influence of processing conditions on plasma parameters and densities of active species; 2) the relationships between fluxes of active species and SiO_2 etching rate; and 3) the analysis of SiO_2 etching mechanisms in terms of the effective reaction probability. The last parameter directly demonstrates what kinds of side factors influence the kinetic of ion-assisted chemical reaction on the treated surface.

EXPERIMENTAL AND MODELING DETAILS

Experimental setup and procedures

Both plasma diagnostics and etching experiments were carried out in the inductively coupled plasma (ICP) reactor described in our previous works [10, 12]. Plasma was excited using the 13.56 MHz power supply matched with the planar copper coil on the top side of the cylindrical reactor chamber. Another 13.56 MHz rf generator powered the bottom electrode to control the negative bias potential, $-U_{\text{dc}}$. The latter was measured using the high-voltage probe (AMN-CTR, Youngsin Eng.). Constant processing conditions were only the total gas flow rate ($q = 40$ sccm) and bias power ($W_{\text{dc}} = 100$ W). Accordingly, variable input parameters were represented by Ar fraction in a feed gas ($y_{\text{Ar}} = 0-75\%$), input power ($W = 400-700$ W that corresponded to $\sim 0.4-0.7$ W/cm³) and gas pressure ($p = 4-10$ mtor).

Electrons- and ions-related plasma parameters were measured using the double Langmuir probe tool (DLP2000, Plasmart Inc.). The treatment of raw I-V curves was based on well-known statements of Langmuir probe theory in low pressure plasmas [4, 13]. Finally, we obtained data on electron temperature (T_e) and ion current density (J_+), and the latter is connected with the total positive ion density as $J_+ \approx 0.61en_+v_B$ [4], where $v_B = (eT_e/m_i)^{1/2}$ is the ion Bohm velocity. The effective ion mass m_i was estimated assuming that the fraction of each ion inside m_i is proportional to $y_i k_{iz,i}$, where y_i is the fraction of corresponding neutral component with the ionization rate coefficient of $k_{iz,i} = f(T_e)$ [14-16].

Etching kinetics of SiO₂ was studied using thermally oxidized Si (111) wafer divided by fragments with an average size of $\sim 2 \times 2$ cm. The small sample size was chosen to exclude the loading effect and thus, to obtain etching rates which adequately reflects heterogeneous process kinetics. Samples were placed in the middle part of the bottom electrode while the temperature of electrode was stabilized at ~ 17 °C using the built-in water-flow cooling system. In order to determine SiO₂ etching rates, a part of sample surface was covered by the photoresist mask (AZ1512, positive) with a thickness of ~ 1.5 μm . Accordingly, after each experiment we measured the step Δh between masked and non-masked areas using the surface profiler Alpha-Step 500 (Tencor) and then, calculated the etching rate as $R = \Delta h/\tau$, where τ is the processing time. Preliminary experiments indicated nearly linear shapes for all kinetic curves $\Delta h = f(\tau)$ within $\tau < 5$ min while longer processing times were found to be undesirable due to the mask damage. Therefore, our experimental conditions surely corresponded to the steady-state etching regime.

Plasma modeling

In order to obtain densities and fluxes of plasma active species, we applied 0-dimensional (global) plasma model operated with volume-averaged plasma parameters. The model content, approaches and kinetic schemes (sets of chemical reactions with corresponding rate coefficients) were the same as have been used in our previous studies of CF₄ + Ar [16-18] and Cl₂ + Ar [16, 19, 20] plasmas under typical RIE conditions. These are gas pressures below 20 mTorr and input power densities ~ 0.1 W/cm³ that corresponds to $n_+ > 10^{10}$ cm⁻³ [4, 5]. Basic assumptions were as follows:

- The electron energy distribution function (EEDF) has the nearly Maxwellian shape [14, 21]. The reason is the high ionization degree for gas species ($n_+/N > 10^{-4}$, where $N = p/k_B T_g$ is the total gas density at the gas temperature of T_g) that provides the essential contribution of equilibrium energy losses in electron-electron collisions. Accordingly, electron-impact rate coefficients were determined using fitting expressions $k = f(T_e)$ [16].

- The gas temperature may be characterized by the nearly constant value at $p, y_{\text{Ar}} = \text{const}$ as well as exhibits the linear growth with input power. Since direct measurements of T_g were not available in this study, our estimation was based on both experimental data provided by Donnelly et al. [17] and the fitting expression $T_g = f(p, W)$ suggested by Thorsteinsson et al. [18]. The latter yields 500–650 K for $W = 400$ –700 W

that looks quite typical for given processing conditions, reactor type and geometry [4].

- The heterogeneous recombination of atoms and radicals appears as the first-order chemical reaction with the rate coefficient of $k \approx (r+l)\gamma v_T/2rl$ [15], where r and l are inner sizes of the cylindrical reactor chamber, v_T is the thermal velocity, and γ is the recombination probability [15, 16].

Though the electronegativity of CF₄ is normally assumed to be low enough for equalizing densities of electrons (n_e) and positive ions (n_+), we applied the identical approach to both gas systems and determined the electron density from measured n_+ using the kinetic equation for negative ions [16]. This allows one to obtain $n_e \approx k_{ii} n_+^2 / (k_{ii} n_+ + k_{da}[X])$, where $k_{ii} \sim 10^{-7}$ cm³/s [14, 16] and $k_{da} = f(T_e)$ [14-16] are rate coefficients for ion-ion recombination and dissociative attachment, respectively. Densities of dominant electronegative components [X] ($X = \text{CF}_4$ for the CF₄ + Ar plasma and $X = \text{Cl}_2$ for the Cl₂ + Ar plasma) were obtained from the solution of chemical kinetic equation for neutral species.

RESULTS AND DISCUSSION

The influence of CF₄/Ar and Cl₂/Ar mixing ratios on electrons- and ions-related plasma parameters as well as on steady-state densities of neutral species have been studied in our previous works [14, 16]. Since most of phenomena have received reasonable explanations, and present data demonstrate the principal agreement with previous ones, we will just briefly summarize the features of these systems with accounting for newly studied effects of gas pressure and input power.

An increase in Ar fraction in a feed gas at $p, W = \text{const}$ causes similar changes in both electron temperature (Fig. 1(a)) and plasma density (Fig. 1(b)). The growth of T_e toward higher y_{Ar} values reflects the increasing fraction of high-energy electrons in EEDF due to a decrease in electron energy losses in inelastic collisions with gas-phase species. The reason is that both CF₄ and Cl₂ molecules (as well as CF_x radicals and Cl atoms as their dissociation products) are characterized by higher cross-sections and lower threshold energies for excitation and ionization processes compared with Ar atoms [24, 25]. Similar increasing tendencies of $n_+ = f(y_{\text{Ar}})$ curves are due to similar changes in ionization reaction kinetics for dominant neutral species, such as R1: CF₄ + e \rightarrow CF₃⁺ + F + 2e, R2: Cl₂ + e \rightarrow Cl₂⁺ + 2e, Cl + e \rightarrow Cl⁺ + 2e and R4: Ar + e \rightarrow Ar⁺ + 2e. The reasons are a) an increase in corresponding rate coefficients together with T_e that results in increasing total ionization frequencies ($k_1[\text{CF}_4] + k_4[\text{Ar}] = 2.8 \cdot 10^4$ – $9.0 \cdot 10^4$ s⁻¹ and $k_2[\text{Cl}_2] + k_3[\text{Cl}] +$

+ $k_4[\text{Ar}] = 5.7 \cdot 10^4 - 9.9 \cdot 10^4 \text{ s}^{-1}$ at 0-75% Ar at $p = 6$ mTorr and $W = 600$ W); and b) the growth of electron density due to decreasing their loss rates in R5: $\text{CF}_4 + e \rightarrow \text{CF}_3 + \text{F}^-$ and R6: $\text{Cl}_2 + e \rightarrow \text{Cl} + \text{Cl}^-$. Since the last process has the threshold-less nature [25], the condition $k_6 \gg k_5$ provides systematically lower n_e values in chlorine-based plasmas. An increase in ion fluxes Γ_+ under the condition of $W_{dc} = \text{const}$ partially compensates for the negative charge on the lower electrode and results in decreasing negative bias voltage ($-U_{dc} = 249-171$ V in $\text{CF}_4 + \text{Ar}$ and $190-144$ V in $\text{Cl}_2 + \text{Ar}$ at 0-75% Ar, $p = 6$ mTorr and $W = 600$ W). At the same time, corresponding changes in ion bombardment energies ε_i being taken under the square root appear to be weaker compared with Γ_+ . That is why the transition toward

Ar-rich plasmas always increases the parameter $(M_i \varepsilon_i)^{1/2} \Gamma_+$ characterizing the ion bombardment intensity (Fig. 1(c)). Decreasing densities (and thus, fluxes) of halogen atoms (Fig. 1(d)) follow changes of their formation rates in R1, R7: $\text{CF}_4 + e \rightarrow \text{CF}_3 + \text{F} + e$; R8: $\text{CF}_3 + e \rightarrow \text{CF}_3 + \text{F} + e$ and R9: $\text{Cl}_2 + e \rightarrow 2\text{Cl} + e$. The slower-than-proportional decrease in both $[\text{F}]$ and $[\text{Cl}]$ (only by ~ 1.2 times for 0-50% Ar) is due to increasing $k_{dis} n_e$ values, where k_{dis} are rate coefficients for above reactions. The condition $[\text{Cl}] \gg [\text{F}]$ mainly follows from differences in dissociation rate coefficients, such as $k_9 \gg k_1 + k_7$. The reason is that R9 exhibits the much lower threshold energy (~ 3 eV compared with 15.9 eV for R1 and 5.6 eV for R7 [14]) and has the higher cross-section for electron energies up to 10 eV.

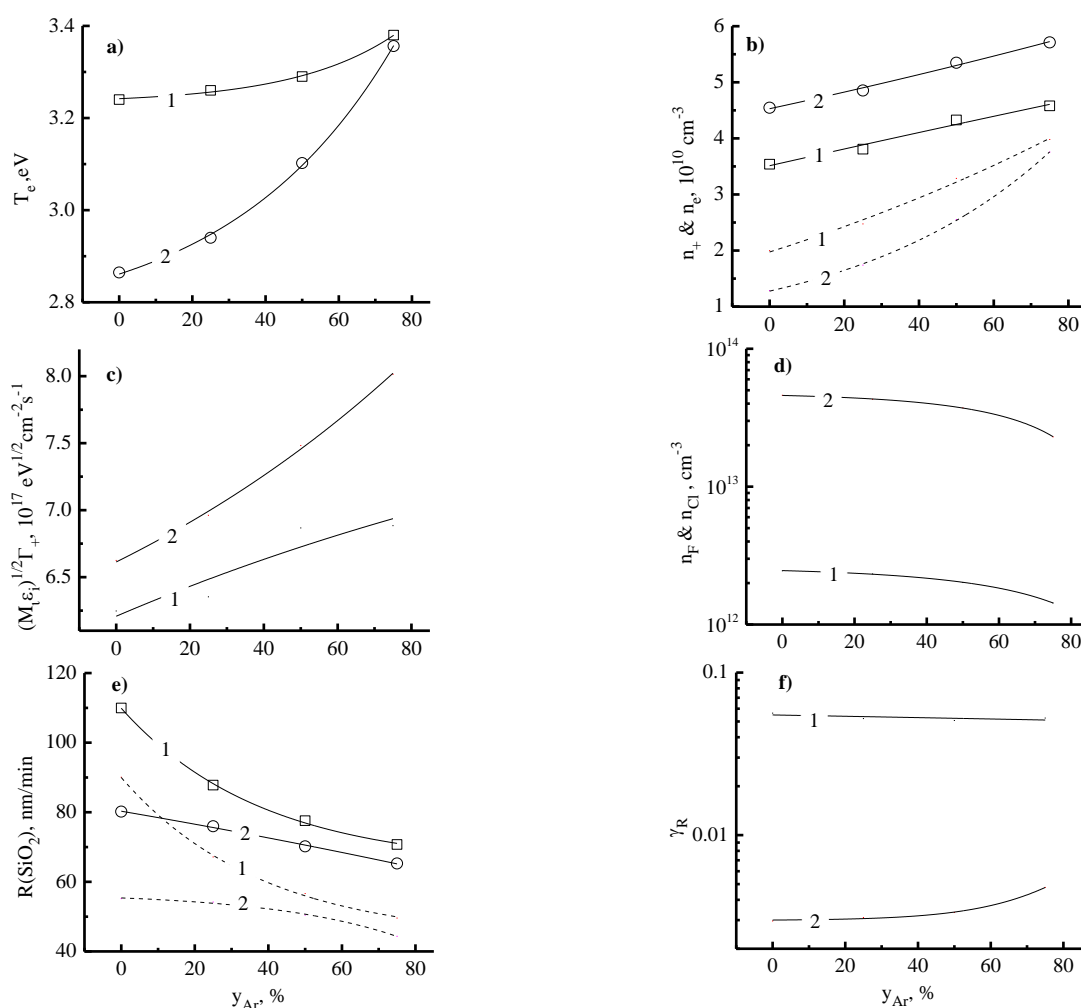


Fig. 1. Plasma parameters, species densities and SiO₂ etching kinetics as functions of Ar fraction in CF₄ + Ar (1) and Cl₂ + Ar (2) mixtures at $p = 6$ mtor and $W = 600$ W: a) electron temperature; b) total positive ion (solid line + symbols) and electron (dashed line) densities; c) parameter $(M_i \varepsilon_i)^{1/2} \Gamma_+$ characterizing the ion bombardment intensity; d) densities of halogen atoms; e) measured SiO₂ etching rate (solid line + symbols) and the rate of heterogeneous chemical reaction (dashed line); and f) effective reaction probability

Рис. 1. Параметры плазмы, концентрации активных частиц и кинетика травления SiO₂ в зависимости от доли Ar в смесях CF₄ + Ar (1) и Cl₂ + Ar (2) при $p = 6$ мтор и $W = 600$ Вт: а) температура электронов; б) суммарная концентрация положительных ионов (сплошная линия + точки) и концентрация электронов (пунктирная линия); в) параметр $(M_i \varepsilon_i)^{1/2} \Gamma_+$ характеризующий интенсивность ионной бомбардировки; д) концентрации атомов галогенов; е) измеренная скорость травления SiO₂ (сплошная линия + точки) и скорость гетерогенной химической реакции (пунктирная линия); и) эффективная вероятность реакции

An increase in input power at y_{Ar} , $p = \text{const}$ causes similar increasing tendencies for both electron temperatures (3.0-3.6 eV in $CF_4 + Ar$ and 2.7-3.2 eV in $Cl_2 + Ar$ at 25% Ar and $p = 6$ mtor, see Fig. 2(a)) and plasma densities ($n_+ = 3.1 \cdot 10^{10}$ - $5.7 \cdot 10^{10} \text{ cm}^{-3}$ in $CF_4 + Ar$ and $4.1 \cdot 10^{10}$ - $7.3 \cdot 10^{10} \text{ cm}^{-3}$ in $Cl_2 + Ar$ at 25% Ar and $p = 6$ mtor, see Fig. 2(b)). The first phenomenon is surely associated with increasing fractions of less saturated radicals and/or atomic species which are characterized by lower electron energy losses compared with original CF_4 or Cl_2 molecules. The second effect in respect to n_e reflects both increases in total ionization frequencies and the limitations of electron loss rates in attachment processes R5 and R6 due to decreasing fractions of multi-atomic electronegative species. Accordingly, the growth of n_+ vs. input power

always follows behaviors of total ionization rates ($R1 + R4$ in $CF_4 + Ar$ and $R2 + R3 + R4$ in $Cl_2 + Ar$). Similarly to the previous case, increasing ion flux overlaps the opposite tendencies for $-U_{dc}$ and thus, enforces the ion bombardment, as shown in Fig. 2(c). From Fig. 2(d), it can be seen also that both F and Cl atoms densities exhibit the monotonic growth toward higher input powers. The evident reason is the acceleration of electron-impact reactions leading to the formation of atomic species. The much weaker change of $[Cl]$ (by ~ 1.5 times for 400-700 W) compared with $[F]$ (by ~ 8 times for 400-700 W) is caused by two reasons, such as 1) the higher dissociation degree of Cl_2 molecules that provides $[Cl] > [Cl_2]$; and 2) the stronger sensitivity of k_1 and k_7 to an increase in T_e due to higher threshold energies compared with R9.

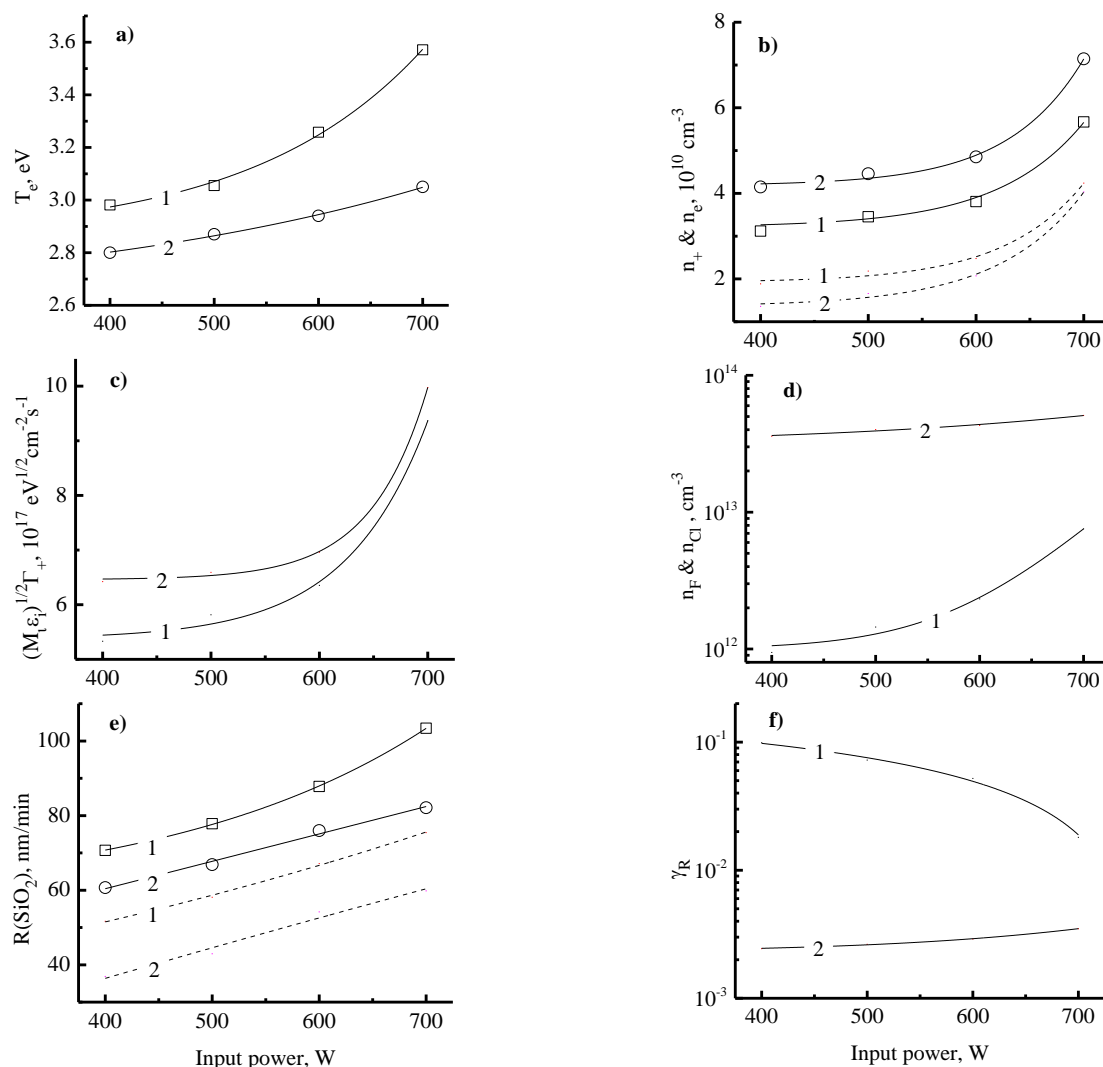


Fig. 2. Plasma parameters, densities of active species and SiO_2 etching kinetics as functions of input power in $CF_4 + Ar$ (1) and $Cl_2 + Ar$ (2) mixtures at $y_{Ar} = 25\%$ and $p = 6$ mtor. Sections a) – f) are identical to fig. 1

Рис. 2. Параметры плазмы, концентрации активных частиц и кинетика травления SiO_2 в зависимости от вкладываемой мощности в смесях $CF_4 + Ar$ (1) и $Cl_2 + Ar$ (2) при $y_{Ar} = 25\%$ и $p = 6$ мтор. Секции а) – ф) идентичны рис. 1

An increase in gas pressure at y_{Ar} , $W = \text{const}$ lowers electron temperatures (3.4-3.0 eV in $\text{CF}_4 + \text{Ar}$ and 3.1-2.8 eV in $\text{Cl}_2 + \text{Ar}$ at 25% Ar and $W = 600 \text{ W}$, see Fig. 3(a)) as well as results in the same effect in respect to plasma densities ($n_+ = 4.5 \cdot 10^{10}$ - $3.1 \cdot 10^{10} \text{ cm}^{-3}$ in $\text{CF}_4 + \text{Ar}$ and $5.5 \cdot 10^{10}$ - $4.3 \cdot 10^{10} \text{ cm}^{-3}$ in $\text{Cl}_2 + \text{Ar}$ at 25% Ar and $W = 600 \text{ W}$, see Fig. 3(b)). Evidently, a decrease in T_e toward higher pressures reflects increasing overall electron energy losses due to increasing electron-neutral collision frequency. Such phenome-

non represents a kind of fundamental rule that takes place in any gas-discharge plasma system [4]. It can be understood also that the growth of gas pressure suppresses the ionization (due to a decrease in ionization rate coefficient for all neutral species) as well as accelerated loss rates for electron in and positive ions in R5, R6 and R10: $\text{F}^+/\text{Cl}^+ + \text{X} \rightarrow \text{F}/\text{Cl} + \text{X}$, where X^+ is any positive ions. Accordingly, the combination of these factors provides monotonically decreasing n_+ and n_e .

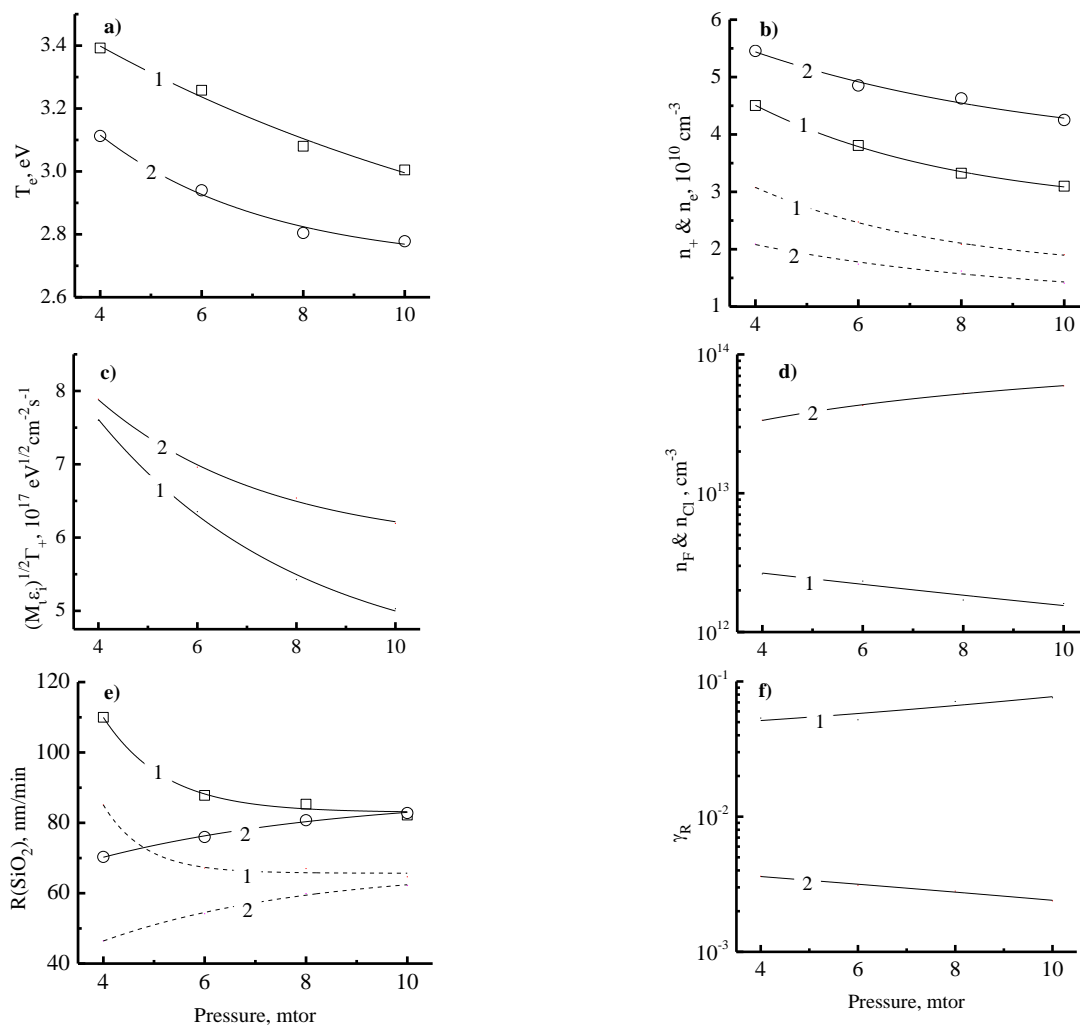


Fig. 3. Plasma parameters, densities of active species and SiO_2 etching kinetics as functions of gas pressure in $\text{CF}_4 + \text{Ar}$ (1) and $\text{Cl}_2 + \text{Ar}$ (2) mixtures at $y_{Ar} = 25\%$ and $W = 600 \text{ W}$. Sections a) – f) are identical to fig. 1

Рис. 3. Параметры плазмы, концентрации активных частиц и кинетика травления SiO_2 в зависимости от давления газа в смесях $\text{CF}_4 + \text{Ar}$ (1) и $\text{Cl}_2 + \text{Ar}$ (2) при $y_{Ar} = 25\%$ и $W = 600 \text{ Вт}$. Секции а) – ф) идентичны рис. 1

The opposite effect of gas pressure on F and Cl atom densities (Fig. 3(d)) is connected with different changes in their formation kinetics. In the $\text{CF}_4 + \text{Ar}$ plasma, a decrease in the dissociative collision frequency for electrons ($(k_1 + k_7)n_e = 10.6$ - 3.1 s^{-1} , or by ~ 3.4 times at $p = 4$ - 10 mtor) overcompensates an increase in $[\text{CF}_4]$ coming with a feed gas. As a result, one

can obtain the monotonic decrease in the F atom formation rate and their density. In the $\text{Cl}_2 + \text{Ar}$ plasma, the dissociation rate coefficient for Cl_2 molecules k_9 is much less sensitive to a decrease of T_e due to lower threshold energy. Such situation produces the weaker fall in $k_9 n_e$ (271 - 162 s^{-1} , or by ~ 1.6 times at $p = 4$ - 10 mtor) as well as provides the increasing tendency for both Cl atom formation rate and $[\text{Cl}]$.

Above data on plasma parameters allow one to divide contributions of physical and chemical etching pathways as well as to suggest the SiO₂ etching mechanism by analyzing correlations between etching kinetics and fluxes of plasma active species. From etching experiments (Figs. 1-3(e)), it was found that 1) the SiO₂ etching rate in both gas systems exhibit similar changes vs. processing parameters, except the effect of gas pressure; and 2) the absolute SiO₂ etching rates in the Cl₂ + Ar plasma (80.2-65.3 nm/min at 0-75% Ar, p = 6 mtor and W = 600 W) are noticeably lower than those in CF₄ + Ar (110.0-70.7 nm/min at 0-75% Ar) under identical processing conditions. Existing experimental data on SiO₂ sputtering yields Y_S vs. the ion bombardment energy (~ 0.13 at ε_i = 200 eV [26, 27]), allow one to estimate the physical sputtering rate as R_{phys} = Y_SΓ₊, and then to extract the chemical etching component (in fact, the rate of ion-assisted chemical reaction) as R_{chem} = R - R_{phys}, where R is the measured etching rate recalculated to the units of particle flux leaving the etched surface. From Figs. 1-3(f), it can be seen that the investigated range of processing conditions surely provides R_{chem} > R_{phys}. The latter means that the dominant etching mechanism in both gas systems is the ion-assisted chemical reaction. Another principal finding is that the change of R_{chem} vs. operating parameters always contradicts with the behavior of (M_iε_i)^{1/2}Γ₊ (in fact, with the ion bombardment intensity), but traces halogen atom fluxes. Formally, such situation means no limitation from the ion-induced process R11: SiO_x(s.) → Si(s.) + xO as well as corresponds to the reaction-rate-limited etching regime which is completely controlled by R12: Si(s.) + xF → SiF_x(s.) or R13: Si(s.) + xCl → SiCl_x(s.) reaction kinetics. At the same time, even a brief look on effective reaction probabilities γ_{R,F} = R_{chem}/Γ_F and γ_{R,Cl} = R_{chem}/Γ_{Cl} (Figs. 1-3(f)), where Γ_F and Γ_{Cl} are fluxes of corresponding halogen atoms, allows one to suggest some differences in above chemical mechanisms. In particular, the behavior of γ_{R,F} always contradicts with the change in (M_iε_i)^{1/2}Γ₊ that reveals either no or even the negative effect of ion bombardment on the rate of R12. The last phenomenon indirectly confirms the spontaneous desorption of reaction products R14: SiF_x(s.) → SiF_x in a form of the high volatile SiF₄ and may be caused by the ion-induced desorption of F atoms under the condition of saturated (i.e. almost completely covered by adsorbed fluorine atoms) surface. It is important to note that the above result is different compared with that obtained in Ref. [12, 28] at higher ion bombardment energies. Both of these reported on the weakly increasing γ_{R,F} together with Ar fraction in a feed gas

and ion bombardment intensity. At the same time, corresponding processing conditions provided the twice higher electron densities, F atoms densities and Γ_F at y_{Ar} < 50%. Probably, the last feature compensates for the ion-induced desorption of F atoms while the more intensive ion bombardment contributes the rate of R14. Oppositely, the parameter γ_{R,Cl} always exhibits much lower absolute values (for example, 6.6·10⁻² vs. 3.0·10⁻³ in pure CF₄ and Cl₂ plasmas, respectively) as well as traces the change in the ion bombardment intensity. The latter means that R13 is activated by the ion bombardment, and the most realistic reason is the production of adsorption sites for chlorine atoms under the condition of low saturated surface. Corresponding ions-related mechanisms are, for example 1) the formation of Si atoms with free bonds through R11; and 2) the desorption of non-saturated low volatile SiCl_x compounds as R15: SiCl_x(s.) → SiCl_x. All these completely confirm as well as reasonably explain the features of SiO₂ etching kinetics in fluorine- and chlorine-based plasmas known from experimental works.

CONCLUSIONS

In this work, we investigated effects of processing conditions (gas mixing ratios, input power and gas pressure) on plasma parameters and reactive-ion etching kinetics for SiO₂ in CF₄ + Ar and Cl₂ + Ar plasmas. It was shown that both gas systems are characterized by similar changes in electron energy and particle balances that provide similar responses in physical and chemical factors influencing the SiO₂ etching rate. The only one exception is the opposite effect of gas pressure on densities of F and Cl atoms originated from corresponding behaviors of their formation rates. The analysis etching kinetics using experimental data on SiO₂ sputtering yields and model-predicted fluxes of plasma active species allowed one to conclude that 1) the dominant etching mechanism in both gas systems is the heterogeneous chemical reaction; 2) both SiO₂ + F and SiO₂ + Cl reaction rates exhibit no limitation by ion-induced processes and correlate with fluxes of fluorine or chlorine atoms; and 3) effective reaction probabilities exhibit opposite changes vs. ion bombardment intensity. The negative effect from the ion bombardment in CF₄ + Ar plasma probably reflects the ion-induced desorption of F atoms under conditions of high their adsorption degree and spontaneous gasification of reaction products. Accordingly, the positive effect in Cl₂ + Ar plasma suggests the ion-induced formation of adsorption sites for Cl atoms under the condition of low volatile reaction products.

The publication was made within the framework of the state task of the Federal State Institution

Scientific Research Institute for System Analysis, Russian Academy of Sciences (conducting fundamental scientific research (47 GP)) on the topic No. 11021060909091-4-1.2.1 "Fundamental and applied research in the field of lithographic limits of semiconductor technologies and physicochemical processes of etching 3D nanometer dielectric structures for the development of critical technologies for the production of electronic components. Research and construction of models and designs of microelectronic elements in an extended temperature range (from -60C to +300C) (FNEF-2022-0006)".

The authors declare the absence a conflict of interest warranting disclosure in this article.

Публикация выполнена в рамках государственного задания ФГУ ФНИЦ НИИСИ РАН (Проведение фундаментальных научных исследований (47 ГП) по теме НИР «11021060909091-4-1.2.1 Фундаментальные и прикладные исследования в области литографических пределов полупроводниковых технологий и физико-химических процессов травления 3D нанометровых диэлектрических структур для развития критических технологий производства ЭКБ. Исследование и построение моделей и конструкций элементов микроэлектроники в расширенном диапазоне температур (от -60C до +300C) (FNEF-2022-0006)».

Авторы заявляют об отсутствии конфликта интересов, требующего раскрытия в данной статье.

REFERENCES ЛИТЕРАТУРА

1. **Nojiri K.** Dry etching technology for semiconductors. Tokyo: Springer Internat. Publ. 2015. 116 p. DOI: 10.1007/978-3-319-10295-5.
2. **Wolf S., Tauber R.N.** Silicon Processing for the VLSI Era. Vol. 1. Process Technology. New York: Lattice Press. 2000. 416 p.
3. Advanced plasma processing technology. New York: John Wiley & Sons Inc. 2008. 479 p.
4. **Lieberman M.A., Lichtenberg A.J.** Principles of plasma discharges and materials processing. New York: John Wiley & Sons Inc. 2005. 757 p. DOI: 10.1002/0471724254.
5. **Donnelly V.M., Kornblit A.** // *J. Vac. Sci. Technol.* 2013. V. 31. P. 050825-48. DOI: 10.1116/1.4819316.
6. **Standaert T.E.F.M., Hedlund C., Joseph E.A., Ohrlein G.S.** // *J. Vac. Sci. Technol. A.* 2004. V. 22. P. 53-60. DOI: 10.1116/1.1626642.
7. **Schaepkens M., Standaert T.E.F.M., Rueger N.R., Sebel P.G.M., Ohrlein G.S., Cook J.M.** // *J. Vac. Sci. Technol. A.* 1999. V. 17. P. 26-37. DOI: 10.1116/1.582108.
8. **Gray D.C., Tepermeister I., Sawin H.H.** // *J. Vac. Sci. Technol. B.* 1993. V. 11. P. 1243-1257. DOI: 10.1116/1.586925.
9. **Vitale S.A., Chae H., Sawin H.H.** // *J. Vac. Sci. Technol.* 2001. V. 19. P. 2197-2206. DOI: 10.1116/1.1378077.
10. **Efremov A., Lee B. J., Kwon K.-H.** // *Materials.* 2021. V. 14. P. 1432(1-27). DOI: 10.3390/ma14061432.
11. CRC Handbook of Chemistry and Physics. New York: CRC Press. 2010. 2760 p.
12. **Efremov A. M., Murin D. B., Betelin V. B., Kwon K.-H.** // *Russ. Microelectronics.* 2020. V. 49. N 2. P. 94-102. DOI: 10.1134/S1063739720010060.
13. **Shun'ko E.V.** Langmuir probe in theory and practice. Boca Raton: Universal Publ. 2008. 245 p.
14. **Kimura T., Ohe K.** // *Plasma Sources Sci. Technol.* 1999. V. 8. P. 553-560. DOI: 10.1088/0963-0252/8/4/305.
15. **Hsu C.C., Nierode M.A., Coburn J.W., Graves D.B.** // *J. Phys. D: Appl. Phys.* 2006. V. 39. P. 3272-3284. DOI: 10.1088/0022-3727/39/15/009.
16. **Efremov A., Lee J., Kwon K.H.** // *Thin Solid Films.* 2017. V. 629. P. 39-48. DOI: 10.1016/j.tsf.2017.03.035.
17. **Efremov A., Murin D., Kwon K.-H.** // *Russ. Microelectronics.* 2020. V. 49. N 3. P. 157-165. DOI: 10.1134/S1063739720020031.
18. **Lim N., Efremov A., Kwon K.-H.** // *Plasma Chem. Plasma Process.* 2021. V. 41. P. 1671-1689. DOI: 10.1007/s11090-021-10198-z.
19. **Efremov A., Min N.K., Choi B.G., Baek K.H., Kwon K.-H.** // *J. Electrochem. Soc.* 2008. V. 155. N 12. P. D777-D782. DOI: 10.1149/1.2993160.
20. **Lee J., Efremov A., Lee B.J., Kwon K.-H.** // *Plasma Chem. Plasma Process.* 2016. V. 36. N 6. P. 1571-1588. DOI: 10.1007/s11090-016-9737-y.
21. **Malyshev M.V., Donnelly V.M.** // *J. Appl. Phys.* 2000. V. 87. P. 1642-1650. DOI: 10.1063/1.372072.
22. **Donnelly V.M., Malyshev M.V.** // *Appl. Phys. Lett.* 2000. V. 77. P. 2467-2470. DOI: 10.1063/1.1318727.
23. **Thorsteinsson E.G., Gudmundsson J.T.** // *Plasma Sources Sci. Technol.* 2010. V. 19. P. 015001 (1-15). DOI: 10.1088/0963-0252/19/1/015001.
24. **Raju G.G.** Gaseous electronics. Tables, Atoms and Molecules. Boca Raton: CRC Press. 2012. 790 p. DOI: 10.1201/b11492.
25. **Christophorou L.G., Olthoff J.K.** Fundamental electron interactions with plasma processing gases. New York: Springer Science+Business Media LLC. 2004. 776 p. DOI: 10.1007/978-1-4419-8971-0.
26. **Seah M.P., Nunney T.S.** // *J. Phys. D: Appl. Phys.* 2010. V. 43. P. 253001 (1-24). DOI: 10.1088/0022-3727/43/25/253001.
27. **Chapman B.** Glow Discharge Processes: Sputtering and Plasma Etching. New York: John Wiley & Sons Inc. 1980. 432 p.
28. **Efremov A.M., Betelin V.B., Mednikov K.A., Kwon K.-H.** // *ChemChemTech [Izv. Vyssh. Uchebn. Zaved. Khim. Khim. Tekhnol.]* 2021. V. 64. N 6. P. 25-34. DOI: 10.6060/ivkkt.20216406.6377.

Поступила в редакцию 17.10.2022

Принята к опубликованию 25.05.2023

Received 17.10.2022

Accepted 25.05.2023